AD-A132 333 A RECTANGULAR GATE MERGED DOSBJT(U) HAWAII UNIV AT MANOA HONOLULU DEPT OF ELECTRICAL ENGINEERING D OKADA ET AL. 1981 N00014-76-C-1081 1/1

UNCLASSIFIED F/G 9/1 NL

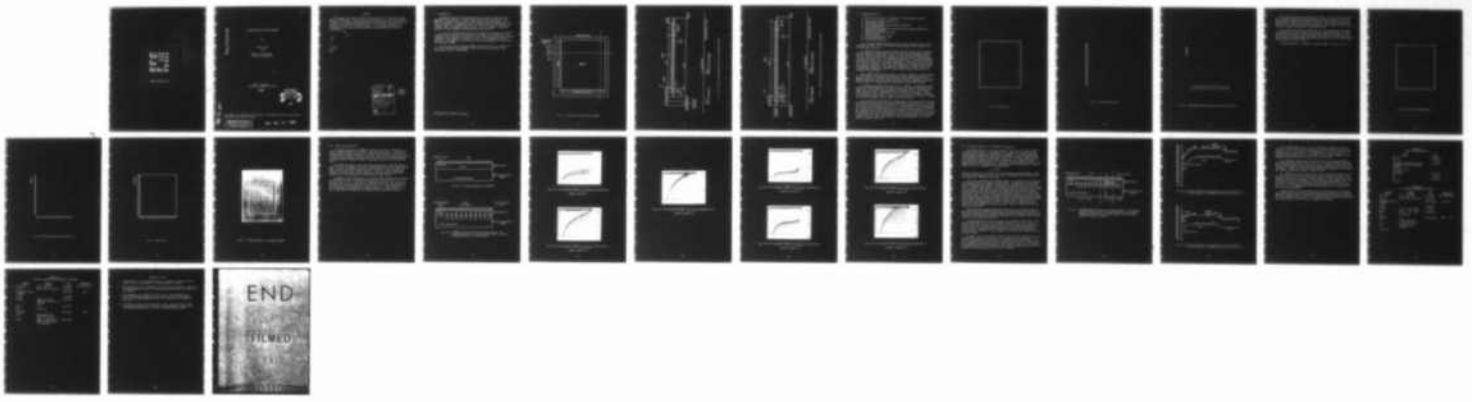

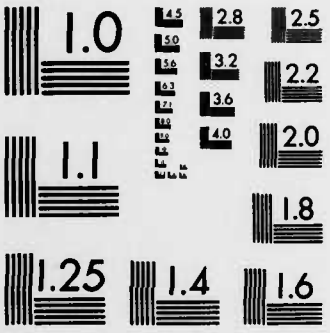

MICROCOPY RESOLUTION TEST CHART
NATIONAL BUREAU OF STANDARDS-1963-A

A RECTANGULAR GATE MERGED MOSBJT*

by

David Okada

and

James W. Holm-Kennedy,
Principal Investigator

ONR Final Report I
Contract No. N00014-76-C-1081

1981

*The MOSBJT was proposed by Prof. James W. Holm-Kennedy, Electrical Engineering Department, University of Hawaii.

ABSTRACT

The design, fabrication and device characteristics of a rectangular gate MOSBJT are described. The characteristics are explained in terms of the merged character of the device and the self biasing effects of the distributed collector current on the collector channel/base bias. For sufficiently high collector currents a portion of the collector channel is self-biased resulting in a decreased β. The active area of the device is then controlled by the device operating bias.

I. Introduction

The MOSBJT* (Metal Oxide Semiconductor Bipolar Junction Transistor) was developed at the University of Hawaii Physical Electronics Laboratory. The MOSBJT is a merged device in which a MOSFET (Metal Oxide Semiconductor Field Effect Transistor) is integrated with a BJT (Bipolar Junction Transistor). The inversion layer of the MOSFET functions as the collector of a BJT resulting in a MOSFET with a distributed bipolar "source." The first MOSBJT's fabricated were of a circular geometry and performed satisfactorily [1].

It will later become evident that the collector/inversion-layer resistivity strongly affects the electrical behavior of the MOSBJT in a complex way. The behavior of the collector/inversion-layer can be significantly varied by changing the MOSBJT's gate geometry. Therefore to aid in the understanding of the opeartion of the MOSBJT a device with an alternate gate geometry was fabricated - the rectangular MOSBJT.

The top view of the rectangular MOSBJT is shown in Fig. 1.1. Figures 1.2 and 1.3 are the front cross-sectional view (AA') and the right-side cross-sectional view (BB'), respectively.

---

*Invented by Dr. James Holm-Kennedy

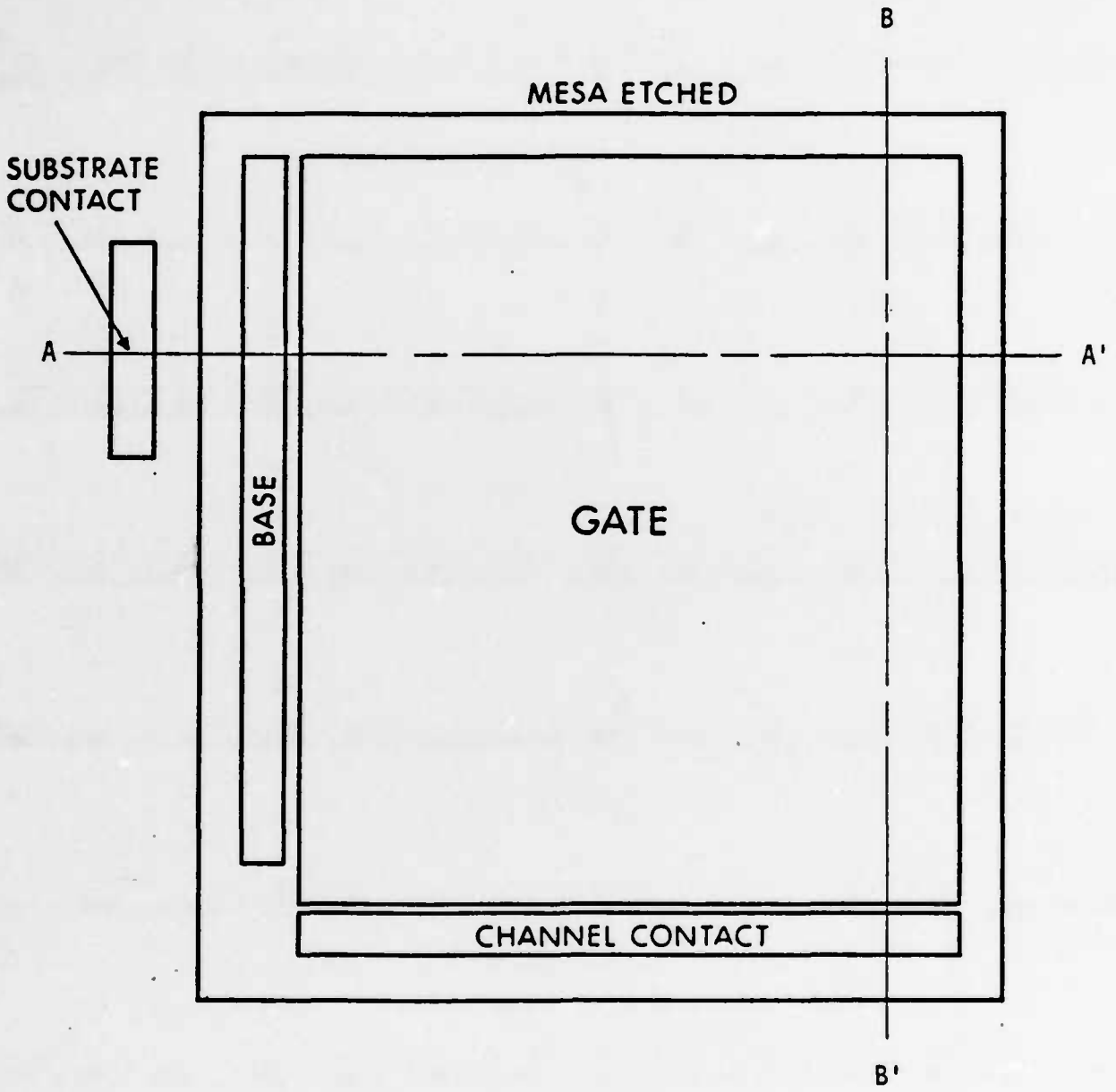

Fig. 1.1 Top View of the Rectangular MOSBJT

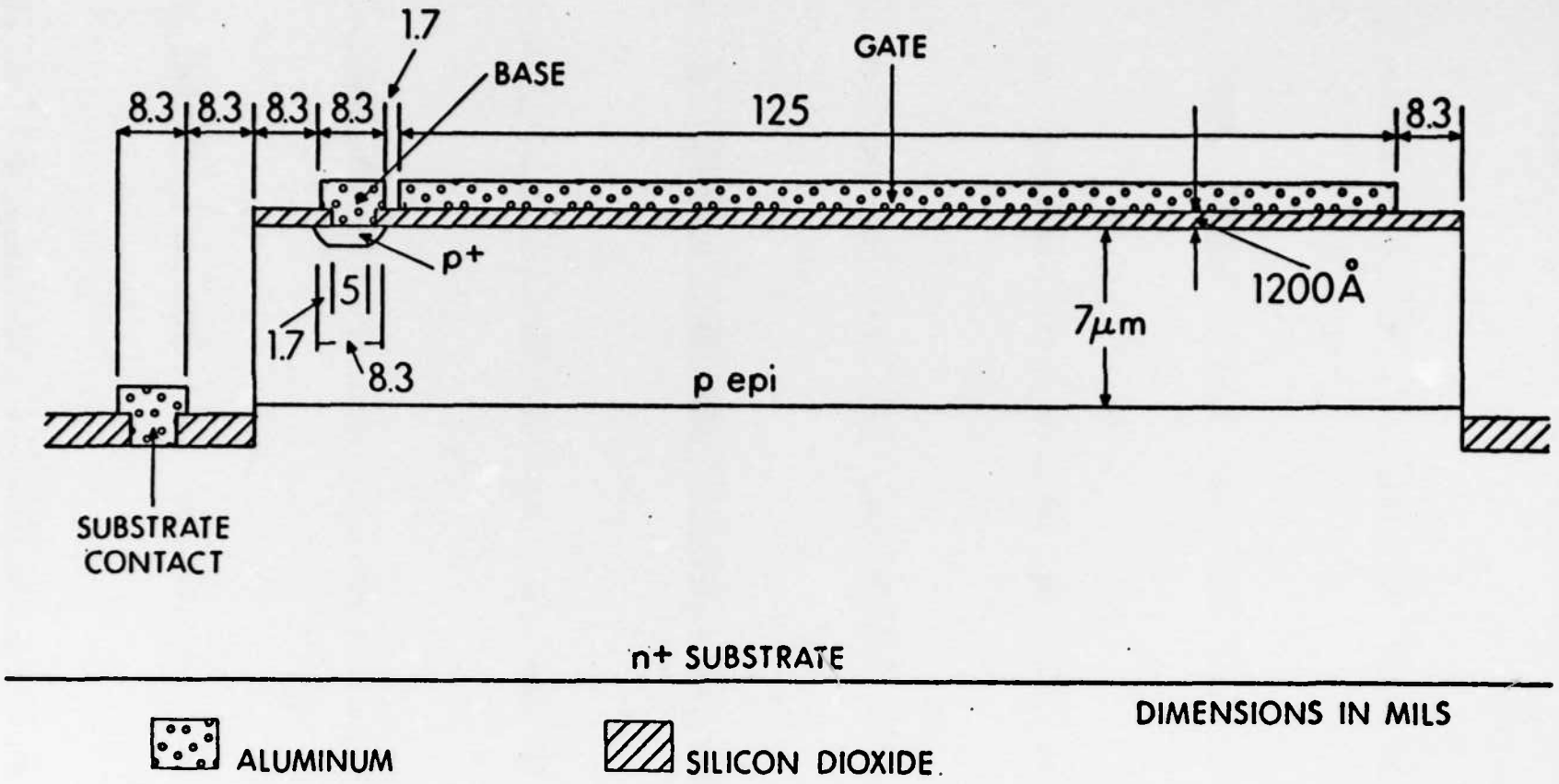

Fig. 1.2 Front cross-sectional view of the rectangular MOSBJT

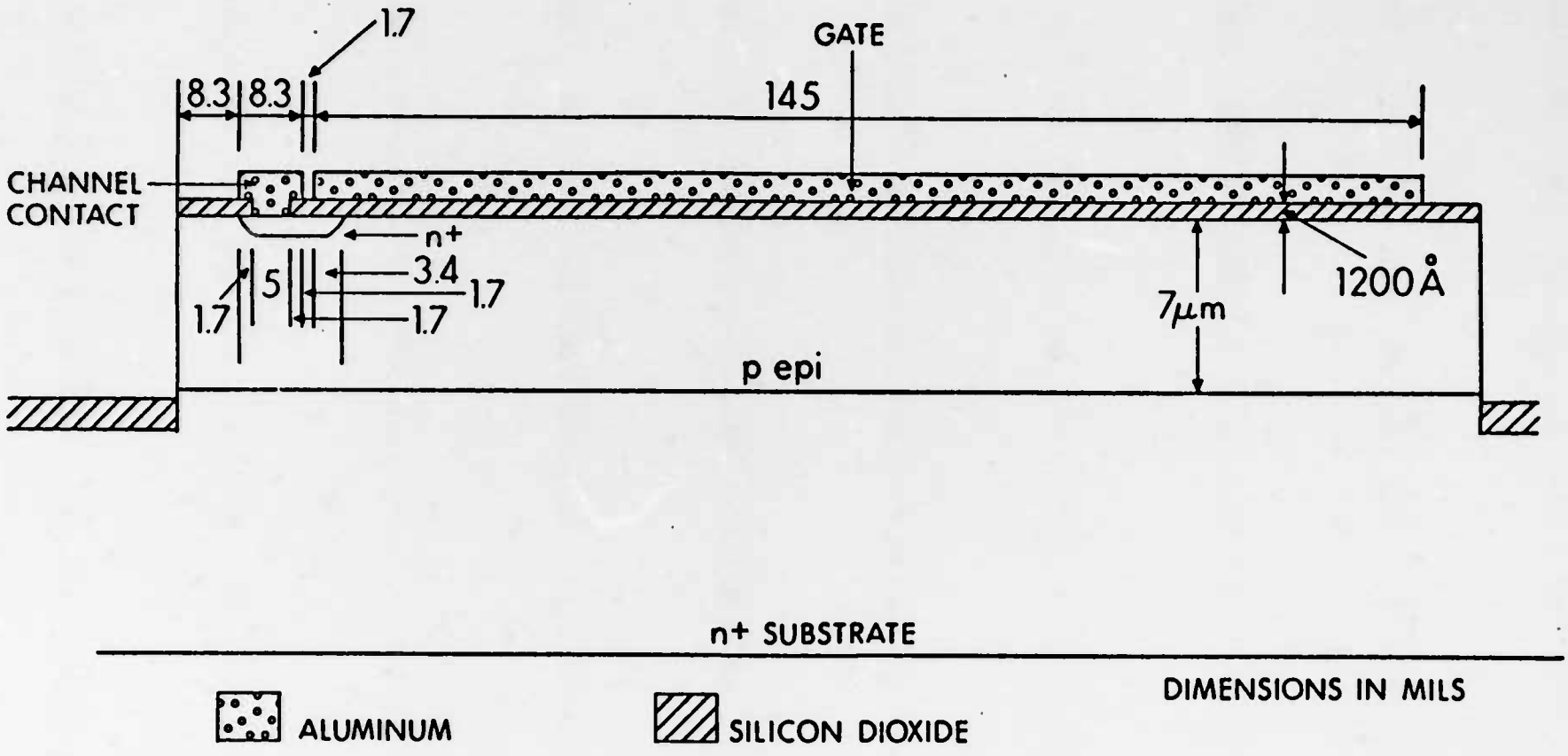

Fig. 1.3 Right-side cross-sectional view of the rectangular MOSBJT

II. Device Fabrication

The fabrication procedure is summarized in the following listing.

1. Define mesa islands and mesa etch
2. Grow blocking oxide
3. Define base contact window and boron diffusion
4. Grow blocking oxide
5. Define emitter/substrate and drain/collector contact windows and phosphorous diffusion
6. Remove existing oxide over gate
7. Grow gate oxide
8. Define metallization windows
9. Aluminum deposition
10. Define metal and sinter

The rectangular MOSBJT was fabricated with <111> oriented silicon wafers consting of a $\sim$7μm, 3.7 Ω-cm resistivity p-type epitaxial layer grown on a n^+ antimony-doped substrate.

To provide electrical isolation of the individual devices and to confine bipolar injection to the channel of the MOS structure the rectangular MOSBJT's were fabricated on silicon mesa islands. The mesa etching procedure was as follows: First the wafers were cleaned (App. A) and the mesa islands defined using the mesa mask (Fig. 2.1) and negative photoresist. The standard negative photoresist procedure (App. B1) was followed and a silicon etchant (Dilute CP-4 1:10::CP-4:DI) was used. To minimize the heating of the etchant and the resultant increase in chemical activity the back surfaces of the wafers were covered with negative photoresist. The wafers were etched for $\sim$1 minute - until the etchant etched through the epitaxial layer thereby forming the electrically isolated silicon islands.

Next a 5000 Å wet oxide was grown (1 hr. 40 min., 1000°C). The base contact was then formed by diffusing boron through an oxide window defined with the negative photoresist procedure (App. B1) and the base diffusion mask (Fig. 2.2). Boron nitride wafers were the dopant source and a 15 min. predeposition was performed at 950°C. A subsequent HF dip removed the surface layer of B_2O_3.

A 1200 Å wet oxide was then grown (15 min., 1000°C). The substrate contact and drain diffusion mask (Fig. 2.3) was used with the negative photoresist procedure (App. B1) to define the phosphorous diffusion windows. The phosphorus source was Emulsitone's Phosphoroscillica (C_S=5x10^{20}) spin-on-dopant. After being spun-on (15 sec., 3000 rpm) the film was cured for 15 minutes at the mouth of the preheated furnace tube. A 950°C, 15 min. predeposition diffusion followed, after which the dopant film was removed with a 10:1 HF dip.

The next step was the growth of the gate oxide. Since the electrical characteristics of MOS devices are significantly affected by the properties of the gate oxide during the fabrication of these devices, strong emphasis was placed on growing a gate oxide of exceptional quality. It is well known that the introduction of chlorine in the oxidizing ambient yields oxides exhibiting superior properties [2]. The addition of small quantities of a common chlorine source TCA (1.1.1. Trichloroethane) into the oxidizing ambient is known to cause significant improvement in oxide properties such as an increase of the average breakdown field strength, reduction of fast surface state density, fixed oxide charge density, and the mobile ion density, etc. [3].

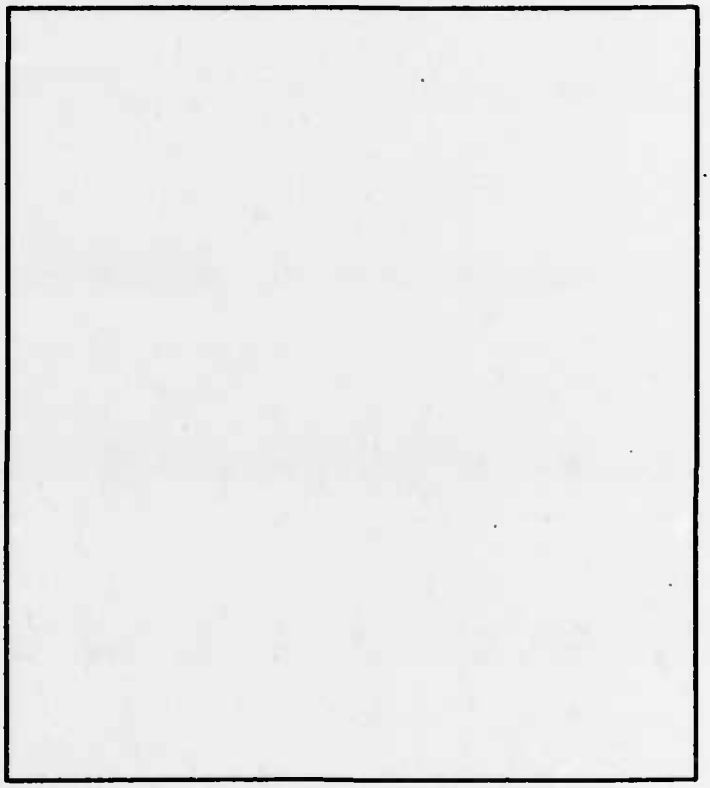

Fig. 2.1 Mesa mask

Fig. 2.2 Base diffusion mask

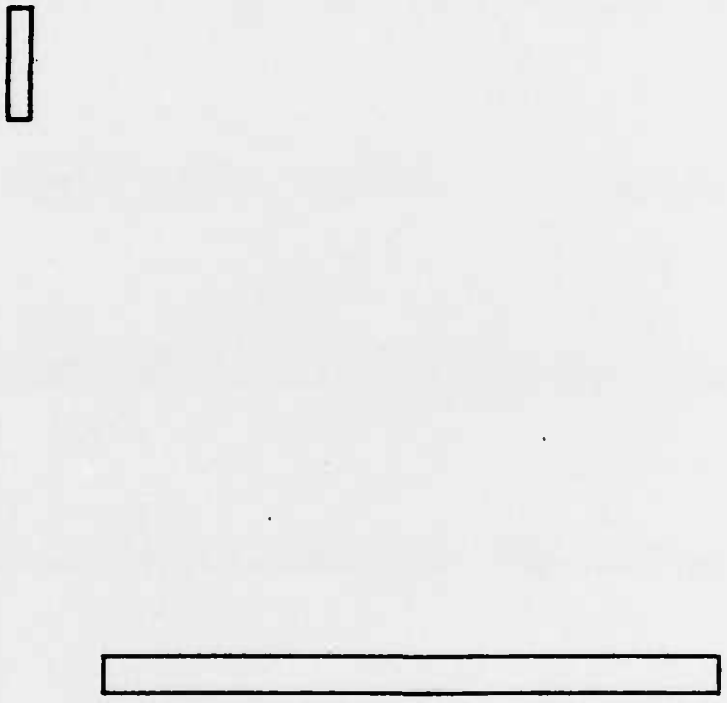

Fig. 2.3 Substrate/emitter contact and drain diffusion mask

The gate oxide growth procedure went as follows: First the existing oxide over the gate region was removed with the gate oxide regrowth mask (Fig. 2.4) and the negative photoresist procedure (App. B1). Next a 1200 Å dry oxide was grown (100 min., 1000°C) in an ambient consisting of dry oxygen and 1% TCA by volume. The oxidation process was followed by a 15 min., 1000°C nitrogen anneal to further reduce the fixed oxide charge density [4].

The negative photoresist procedure (App. B1) and the metallization contact window mask (Fig. 2.5) were used to open windows in the oxide layer. Aluminum was then evaporated onto the wafer surface at a pressure of 1×10^{-6} torr. The definition of the aluminum gate and contact pads were carried out using the positive photoresist procedure (App. B2) and the metal mask (Fig. 2.6). The devices were sintered for 5 min. at 450°C.

A photomicrograph of a completed rectangular MOSBJT is shown in Fig. 2.7.

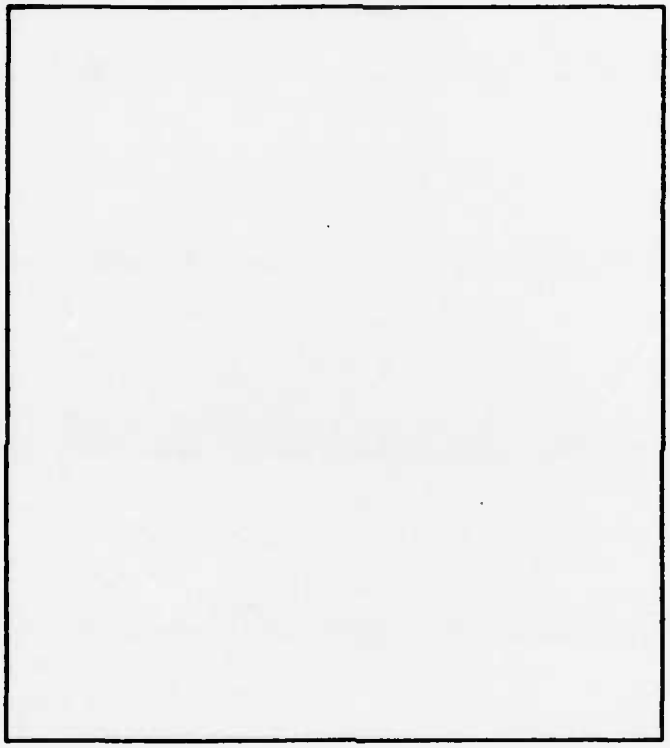

Fig. 2.4 Gate oxide regrowth mask

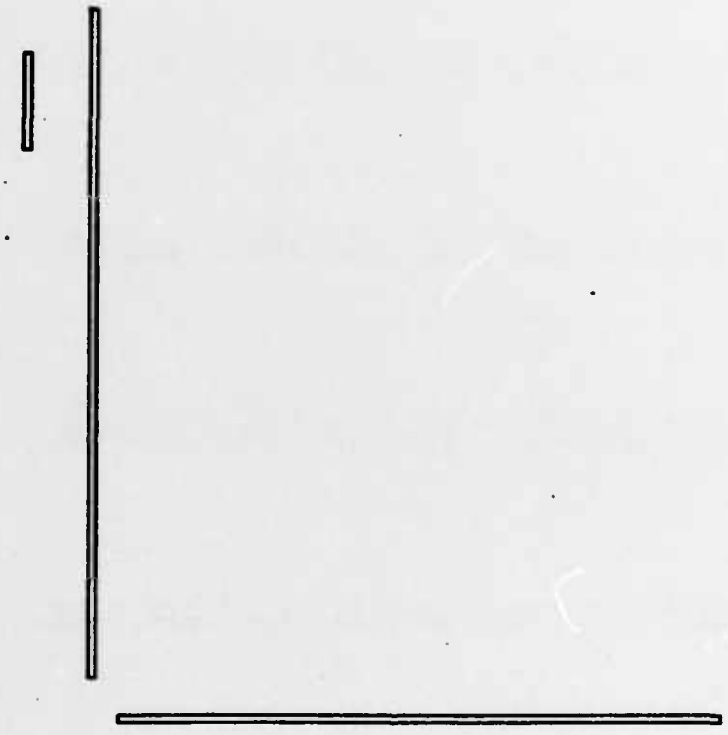

Fig. 2.5 Metallization contact window mask

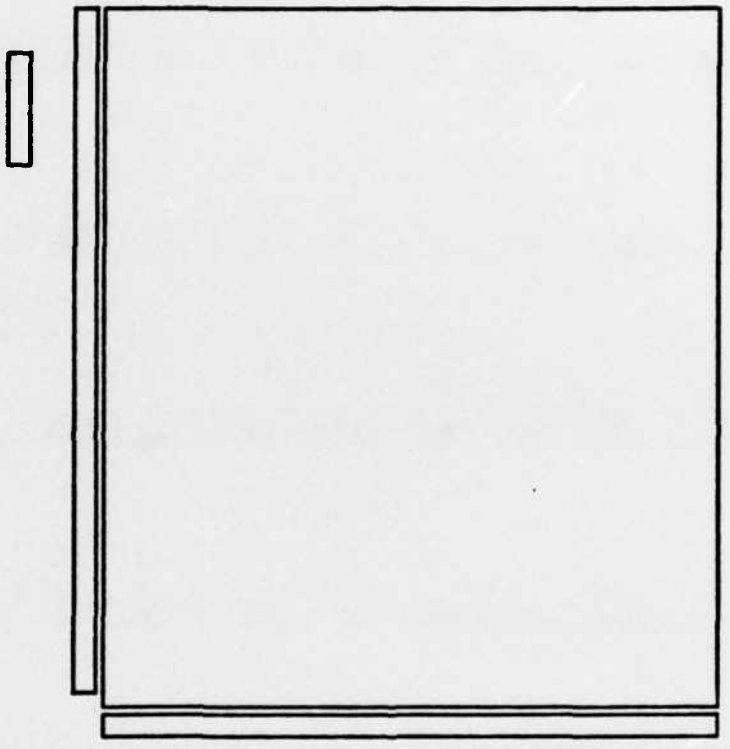

Fig. 2.6 Metal mask

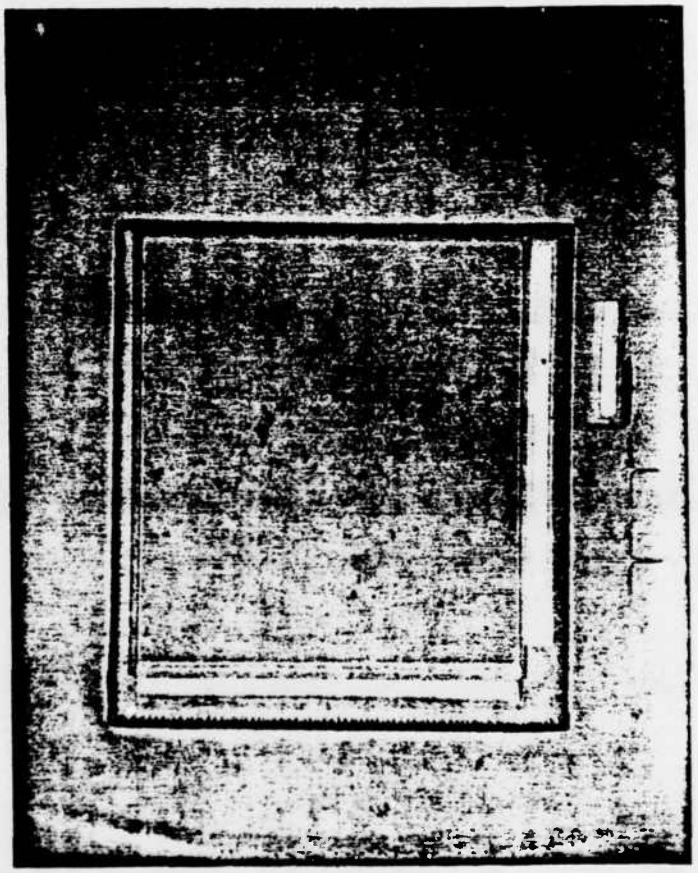

Fig. 2.7 Photomicrograph of a rectangular MOSBJT

III. Device Characterization

A simplified diagram of the MOSBJT is shown in Fig. 3.1a. Figure 3.1b reveals a MOSBJT biased in the forward active mode of operation. In the forward active mode the emitter-base junction is forward biased resulting in electron injection into the base from the n^+ substrate. The inversion layer-base junction is reverse biased thereby functioning as a "collector" for the injected electrons. The drain/collector contact provides an electrical connection to the inversion layer.

The MOSBJT operating in the forward active mode has the same bias requirements as a n-p-n BJT (Bipolar Junction Transistor) operating in the forward active mode. Therefore the MOSBJT can be characterized with an I-V curve-tracer configured to test BJTs with an added gate bias. The base current step generator controls the emitter-base junction forward bias and the inversion layer-base junction bias is provided by the collector-emitter sweep voltage.

The MOSBJT's "BJT" characteristics (collector/drain current versus collector/drain-emitter voltage for various base currents) are shown in Figs. 3.2a, b, c and Figs. 3.3a, b, c, d. The set of I-V characterstics (Figs. 3.2a, b, c) are recorded with the gate voltage (V_G) kept constant at 20V while the magnitude of the base current steps were varied. Figures 3.3a, b, c, d show the effect of gate voltage (V_G) on the MOSBJT's BJT characteristics. In Figs. 3.3a, b, c, d V_G is varied while the magnitude of the base current steps remain constant.

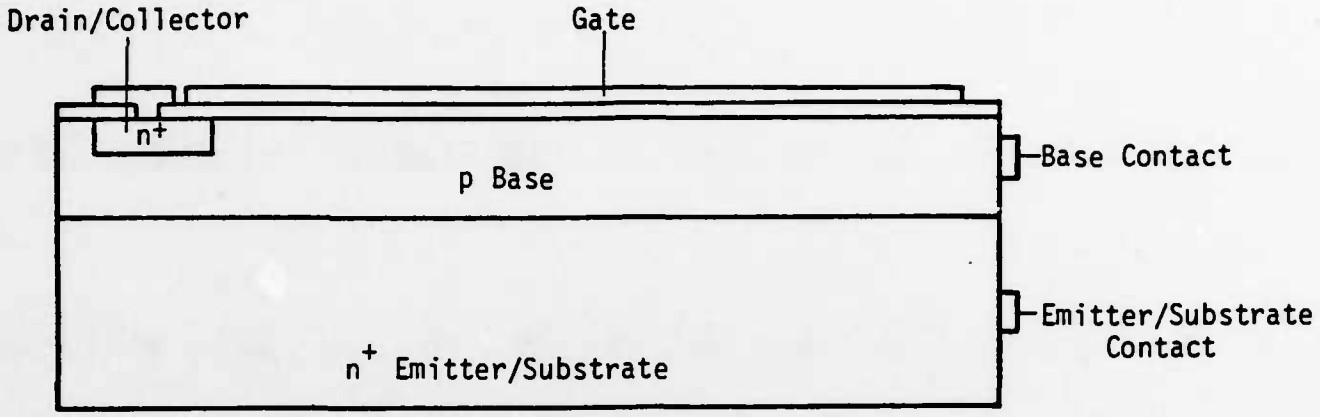

Fig. 3.1a A simplified model of the MOSBJT

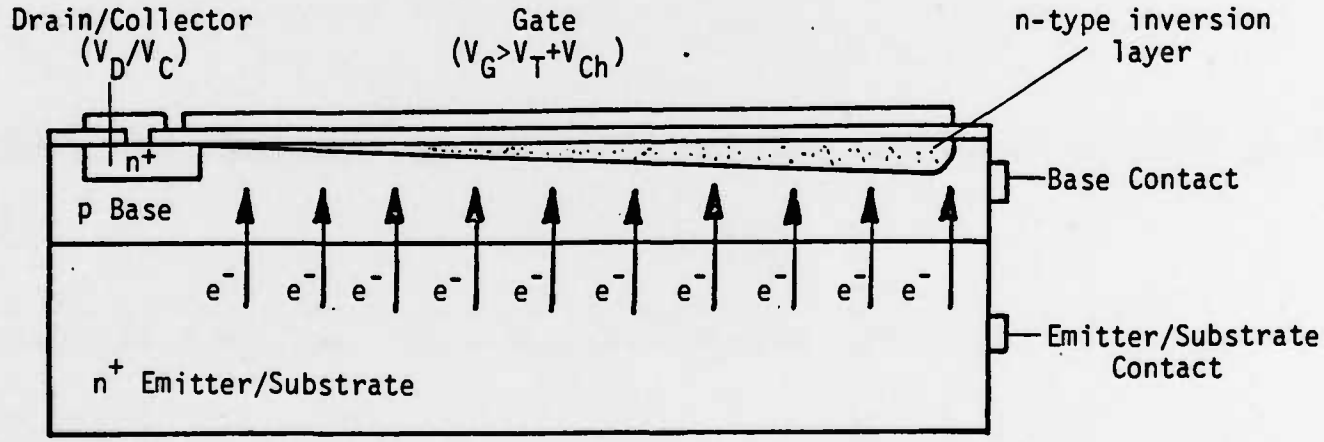

Fig. 3.1b A MOSBJT biased into the forward active regime. The emitter/base junction is forward biased and the inversion layer-base junction is reverse biased.

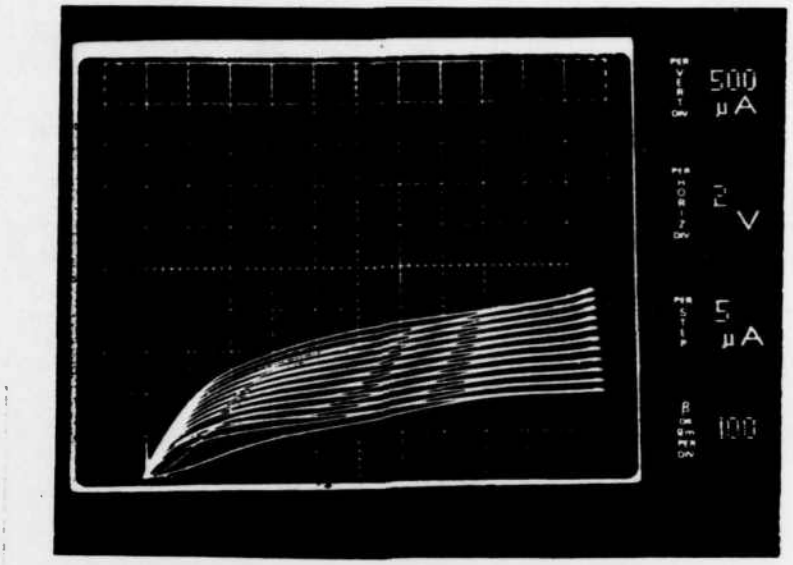

Fig. 3.2a The rectangular MOSBJT I_D/I_C-V_{DE}/V_{CE} characteristics

V_G=20V, ΔI_B=5.0 μA

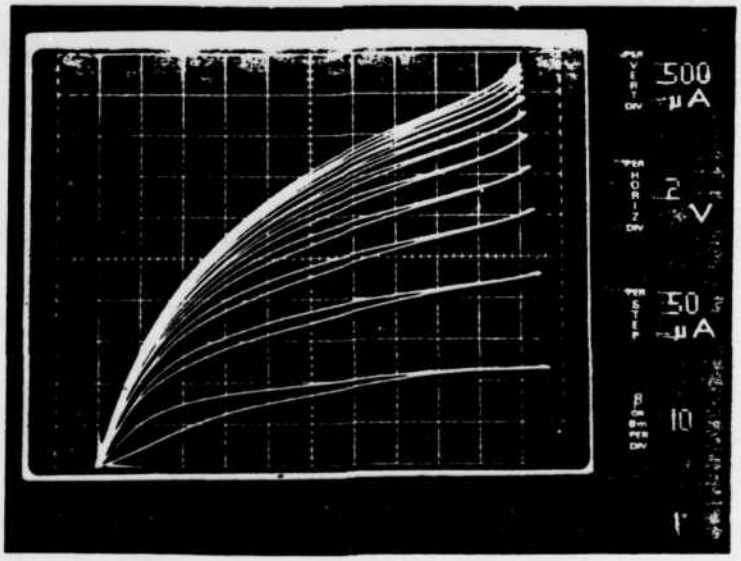

Fig. 3.2b The rectangular MOSBJT I_D/I_C-V_{DE}/V_{CE} characteristics

V_G=20V, ΔI_B=50.0 μA

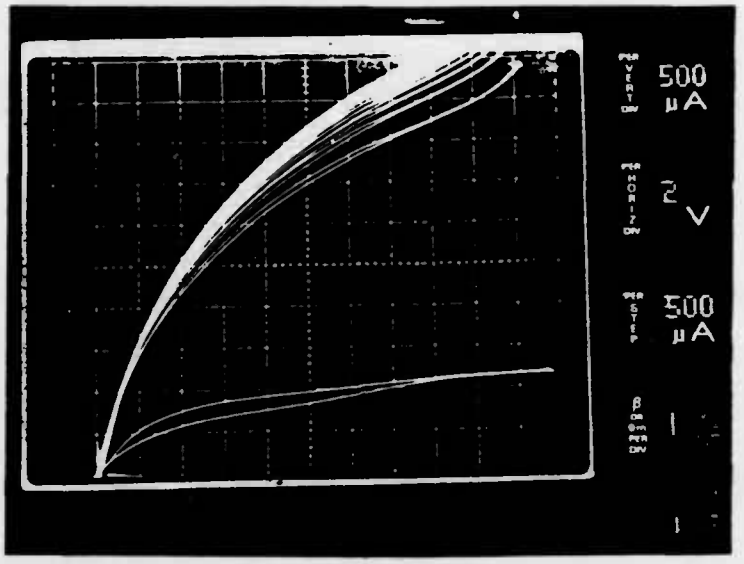

Fig. 3.2c The rectangular MOSBJT I_D/I_C-V_{DE}/V_{CE} characteristics

V_G=20V, ΔI_B=500.0 μA

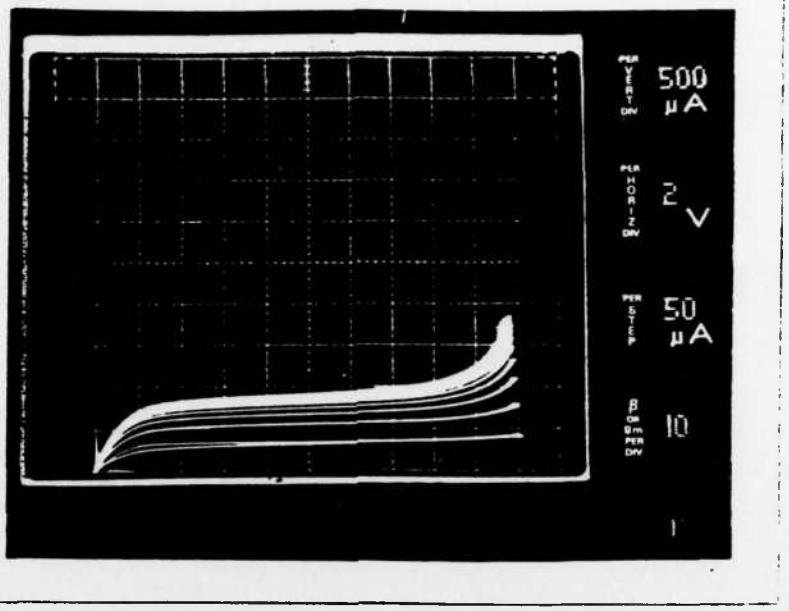

Fig. 3.3a The rectangular MOSBJT I_D/I_C-V_{DE}/V_{CE} characteristics

V_G=0.0V, ΔI_B =50.0 μA

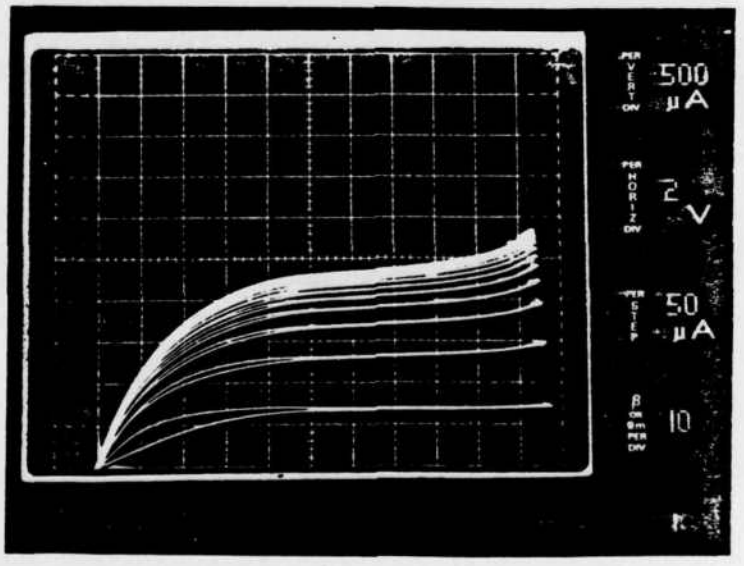

Fig. 3.3b The rectangular MOSBJT I_D/I_C-V_{DE}/V_{CE} characteristics

V_G=10.0V, ΔI_B=50.0 μA

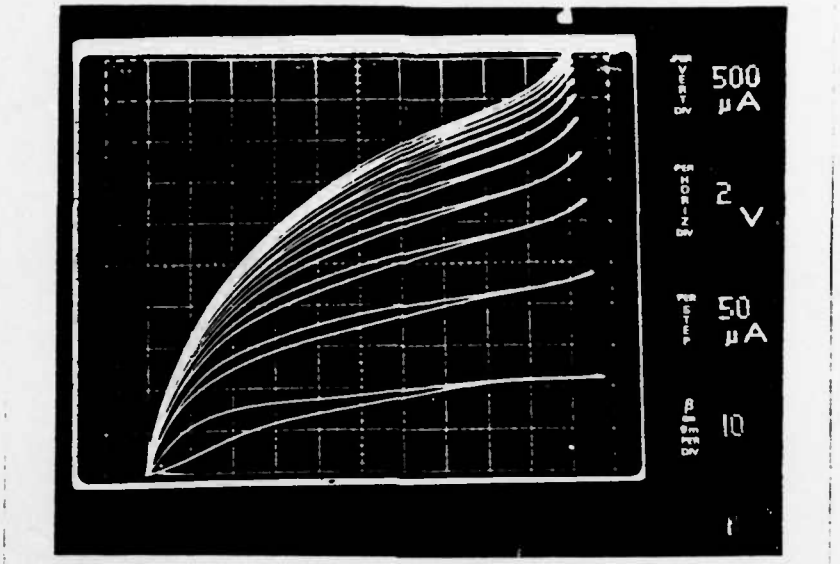

Fig. 3.3c The rectangular MOSBJT I_D/I_C-V_{DE}/V_{CE} characteristics

V_G=20.0V, ΔI_B=50.0 μA

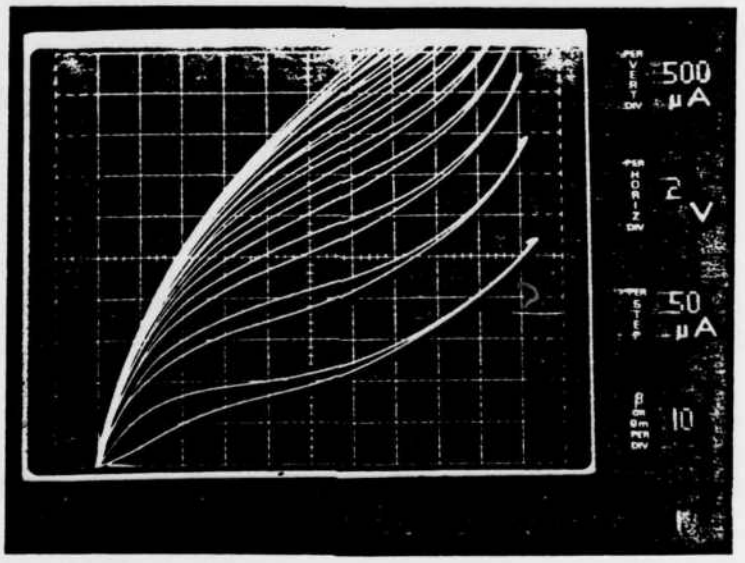

Fig. 3.3d The rectangular MOSBJT I_D/I_C-V_{DE}/V_{CE} characteristics

V_G=30.0V, ΔI_B=50.0 μA

IV. Qualitative Analysis of the MOSBJT's I_D/I_C-V_{DE}/V_{CE}

As evident from Figs. 3.2a, b, c and Figs. 3.3a, b, c, d, the most unusual electrical characteristic of the MSOBJT is the saturation of collector/drain current (I_D/I_C) as the base current (I_B) is increased. To properly understand this phenomena consider the simplified cross-sectional view of a MOSBJT biased into the "forward active" regime shown in Fig. 3.1b. The emitter-base junction of the MOSBJT is biased at a low level of injection (low injection) and the entire inversion layer operates as a "collector" for the injected electrons. The MOSBJT biased into a "low-injection," "forward-active" mode operates in a manner similar to a BJT. Therefore it is expected that

$$I_C \approx \beta I_B \ .$$

The above expression is consistent with the observed rectangular MOSBJT's characteristics (I_D/I_C-V_{DE}/V_{CE}) (Fig. 3.2a) in which the MOSBJT has been biased into a "low injection," "forward active" mode.

In the "low injection" case discussed above it is assumed that the inversion layer-base junction is everywhere reverse biased. As the forward bias voltage on the emitter-base junction (V_{BE}) is increased this assumption may no longer be valid. Increasing V_{BE} results in the increase of electron injection into the base and an increase in the number of carriers collected by the inversion layer. Once in the inversion layer the electrons drift toward the drain/collector contact. The electron flow along the resistive inversion layer results in a voltage drop along the channel. As V_{BE} is increased, sufficient voltage drop may occur along the inversion layer such that the region furthest from the drain/collector contact is no longer adequately reverse biased as it must to efficiently collect electrons. (This region will be referred to as the "cut-off" region. The onset of this action will be referred to as "cut-off.") Figure 4.1 is a simplified cross-sectional view of a MOSBJT biased into cut-off. Both the "active" and "cut-off" regions are indicated.

Figure 4.2a shows the band diagram for the vertical n-p-n BJT structure of the active region of a MOSBJT biased into cut-off (along Section AA' in Fig. 4.1). The emitter-base junction is forward biased resulting in electron injection into the base. The electrons diffuse across the base and are collected by the reverse-biased inversion-layer-base junction.

The band diagram for the vertical n-p-n BJT structure of the cut-off region (along Section BB' in Fig. 4.1) of a MOSBJT is shown in Fig. 4.2b. In the cut-off region self-forward biasing of the inversion layer-base junction results in the vertical BJT structure being biased into a unique saturated condition. The saturation is characterized by a constant minority carrier concentration across the base resulting in no net transport of carriers from the emitter to the inversion layer.

As shown in Fig. 4.1 electrons injected into the cut-off region must diffuse to the active region to be collected. This increases the "path length" or "effective base width" for the electrons injected into the cut-off region, resulting in increased recombination of the carriers injected into the cut-off region. The recombination of injected electrons in the base may reduce the collector/drain current density and increase the base current. Both of these effects result in a reduction of the bipolar current gain (β) of the MOSBJT.

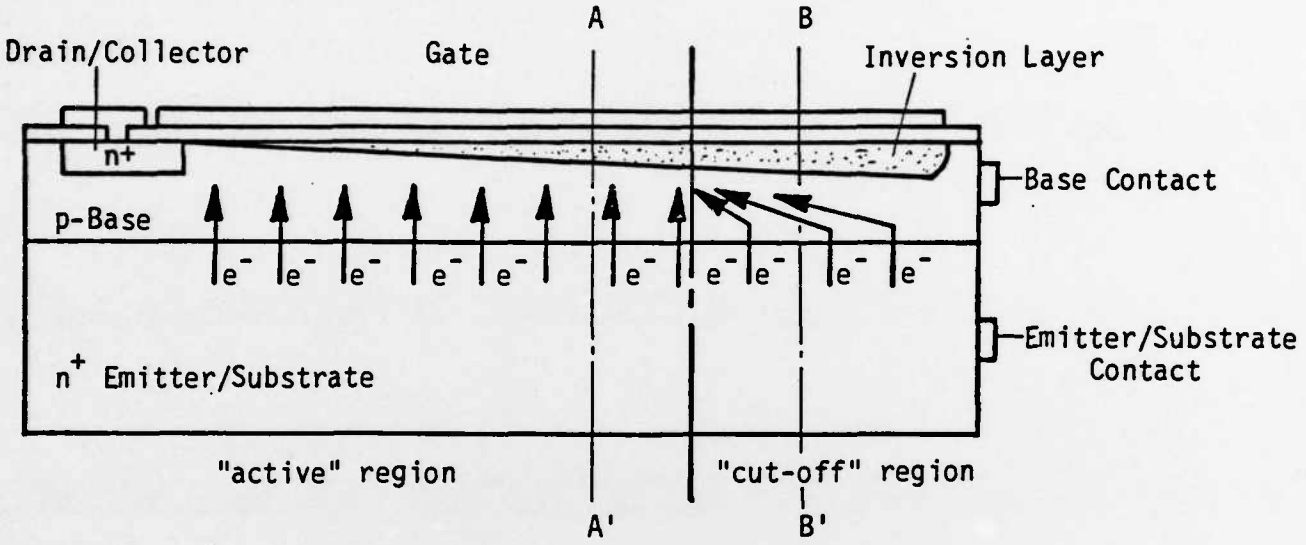

Fig. 4.1 A MOSBJT biased into the cut-off operating mode. In this mode the emitter-base junction is forward biased but the inversion layer-base junction in the cut-off region is insufficiently biased to "collect" electrons.

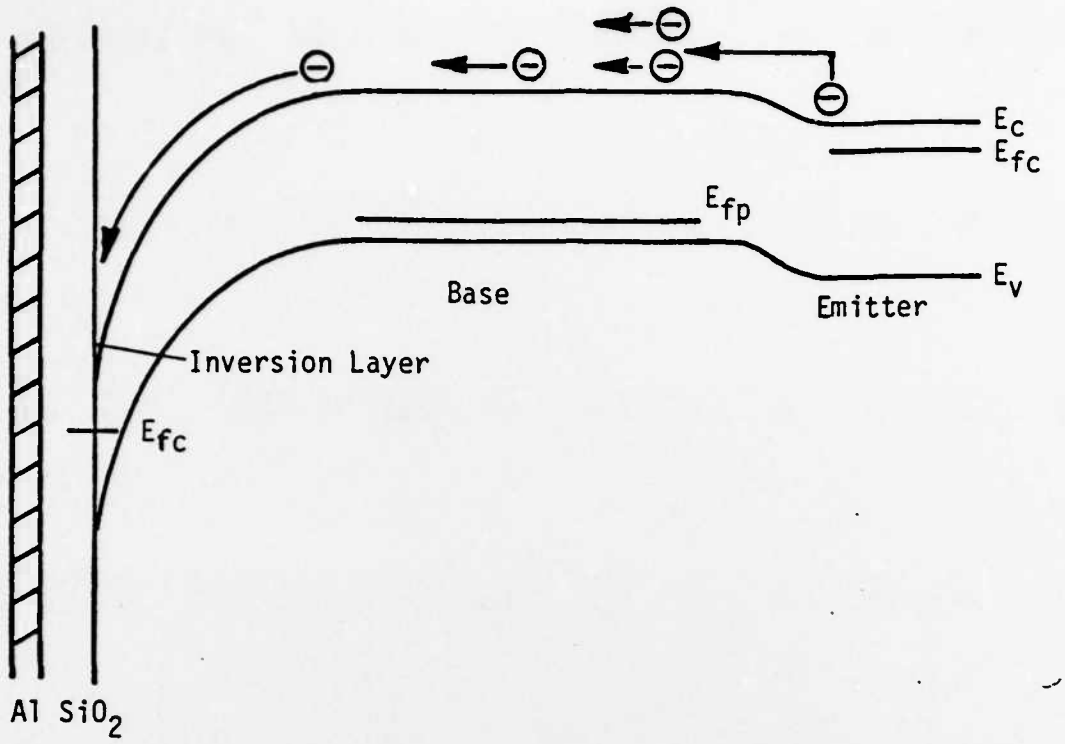

Fig. 4.2a The band diagram for the vertical n-p-n BJT structure of the active region of a MOSBJT biased into cut-off (Fig. 4.1).

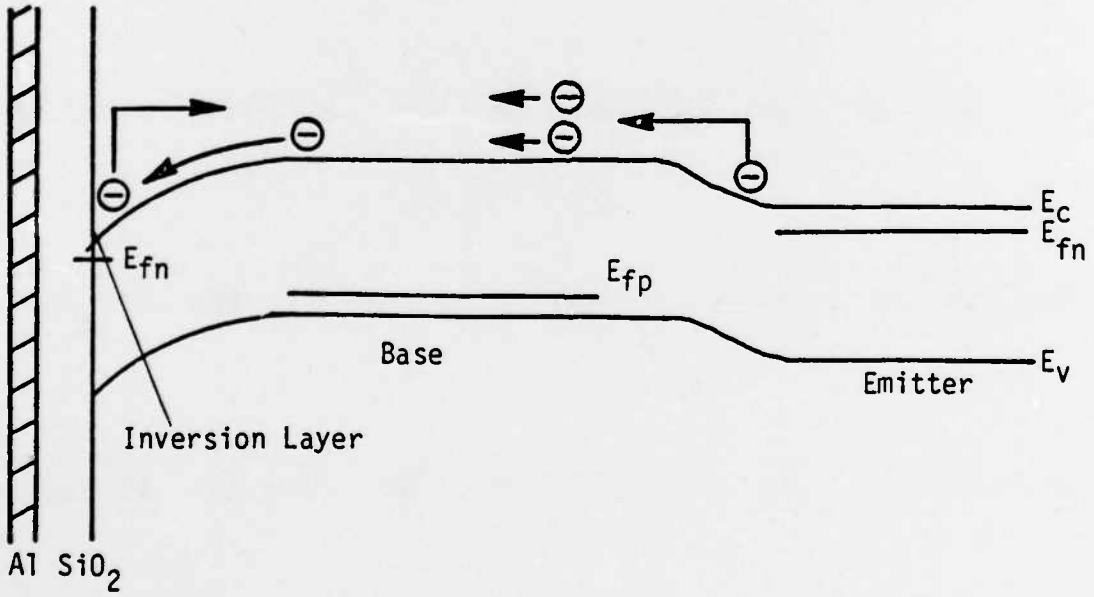

Fig. 4.2b The band diagram for the vertical n-p-n BJT structure of the cut-off region of a MOSBJT biased into cut-off (Fig. 4.1).

For the MOSBJT biased into cut-off, increasing I_B increases the current collected by the inversion layer resulting in a greater voltage drop along the channel. This in turn results in the lengthening of the cut-off region and the associated further reduction of β. The reduction of β as I_B increases is responsible for collector current saturation in the rectangular MOSBJT's I_D/I_C-V_{DE}/V_{CE} characteristics (Figs. 3.2b, c, Fig. 3.3a, b, c, d).

The significant effect gate voltage (V_G) has on the rectangular MOSBJT I_D/I_C-V_{DE}/V_{CE} characteristics (Figs. 3.3a, b, c, d) results from the dependence of the inversion-layer resistivity on V_G. As V_G is increased (while I_B is kept constant) the channel restivity decreases thereby reducing the voltage drop along the channel. Therefore a larger I_B is required before the MOSBJT is self-biased into cut-off and collector current saturation occurs.

For a MOSBJT biased into cut-off with a channel length much greater than the base minority carrier diffusion length $L_n \approx 30$ m) a substantial fraction of the electrons injected into the cut-off region recombines. This results in a rapid reduction in β as I_B is increased. The fabricated rectangular MOSBJT has a channel length of $\sim$3600 μm and therefore the very pronounced collector current saturation in the device's I_D/I_C-V_{DE}/V_{CE} characteristics (Figs. 3.2b, c, Figs. 3.3a, b, c, d) is consistent with the current understanding of the operation of the "forward active" MOSBJT.

The non-linearities arising from the active area modulation, its effects on base current and β have many useful applications which include mixing, harmonic generation, amplification. The details of the applications are being studied and will be described at a later date. It is believed that the active area modulation with bias of the BJT or FET was first proposed by the authors.

APPENDIX A
WAFER CLEANING PROCEDURE

Process	Time
10:1 HF	10 seconds
DI rinse	2 minutes
Ultrasonic agitation and gentle scrubbing in a hot Acationox/DI solution	2 minutes
Thorough DI rinse	
H_2SO_4/H_2O_2	5 minutes
DI	5 minutes
DI	10 minutes
Spin dry	

APPENDIX B1
KTI NEGATIVE PHOTORESIST PROCEDURE

Process	Method	Time	Temperature
Coat wafer	Spin at 4000 RPM	15 seconds	Room temperature
Air dry	Under laminar flow hood	3 minutes	
Prebake the resist coating		25±5 minutes	90 ± 5°C
Expose		6 seconds	
Develop	Soak in KTI developer	1 minute	
Rinse	Immerse in KTI rinse	30 seconds	
Dry	N_2 blow dry		
Postbake		25±5 minutes	140°C ± 5°C
Etch	Immerse into the appropriate etchant		
Strip	Using H_2SO_4/H_2O_2 solution		
Clean wafer			

APPENDIX B2
SHIPLEY AZ-1360J POSITIVE PHOTORESIST PROCEDURE

Process	Method	Time	Temperature
Coat wafer	Spin at 4000 RPM	15 seconds	Room temperature
Air dry	Under laminar flow hood	3 minutes	
Prebake the resist coating		15 minutes	100°C
Expose		6 seconds	
Develop	Immerse in AZ-606 developer diluted 10:1 with DI	25 seconds	
Rinse	In DI	10 seconds	
Dry	N_2 blow dry		
Postbake		15 minutes	95°C
Etch	Immerse into the appropriate etchant		
Strip	Immerse in Shipley remover--1112A diluted 2:1::DI:1112A	30 seconds	

References Cited

1. "Fabrication of a Silicon MOSFET Device with a Bipolar Transistor Source," Master's Thesis, David Okada, Dec. 1979, University of Hawaii.

2. B.R. Singh and P. Balk, "Oxidation of Silicon in the Presence of Chlorine and Chlorine Compounds," Journal of the Electrochemical Society, Vol. 125, No. 3, pp. 453-461.

3. E.J. Jansenns, G.J. Declerck, "The Use of 1.1.1. Trichloroethane as an Optimized Additive to Improved Silicon Thermal Oxidation Technology," Journal of the Electrochemical Society, Vol. 125, No. 10, pp. 1696-1703, Oct. 1978.

4. B.E. Deal, M. Sklar, A.S. Grove, and E.H. Snow, "Characteristics of the Surface-State Charge (QSS) of Thermally Oxidized Silicon," Journal of the Electrochemical Society, Vol. 114, No. 3, pp. 226-274, March 1976.

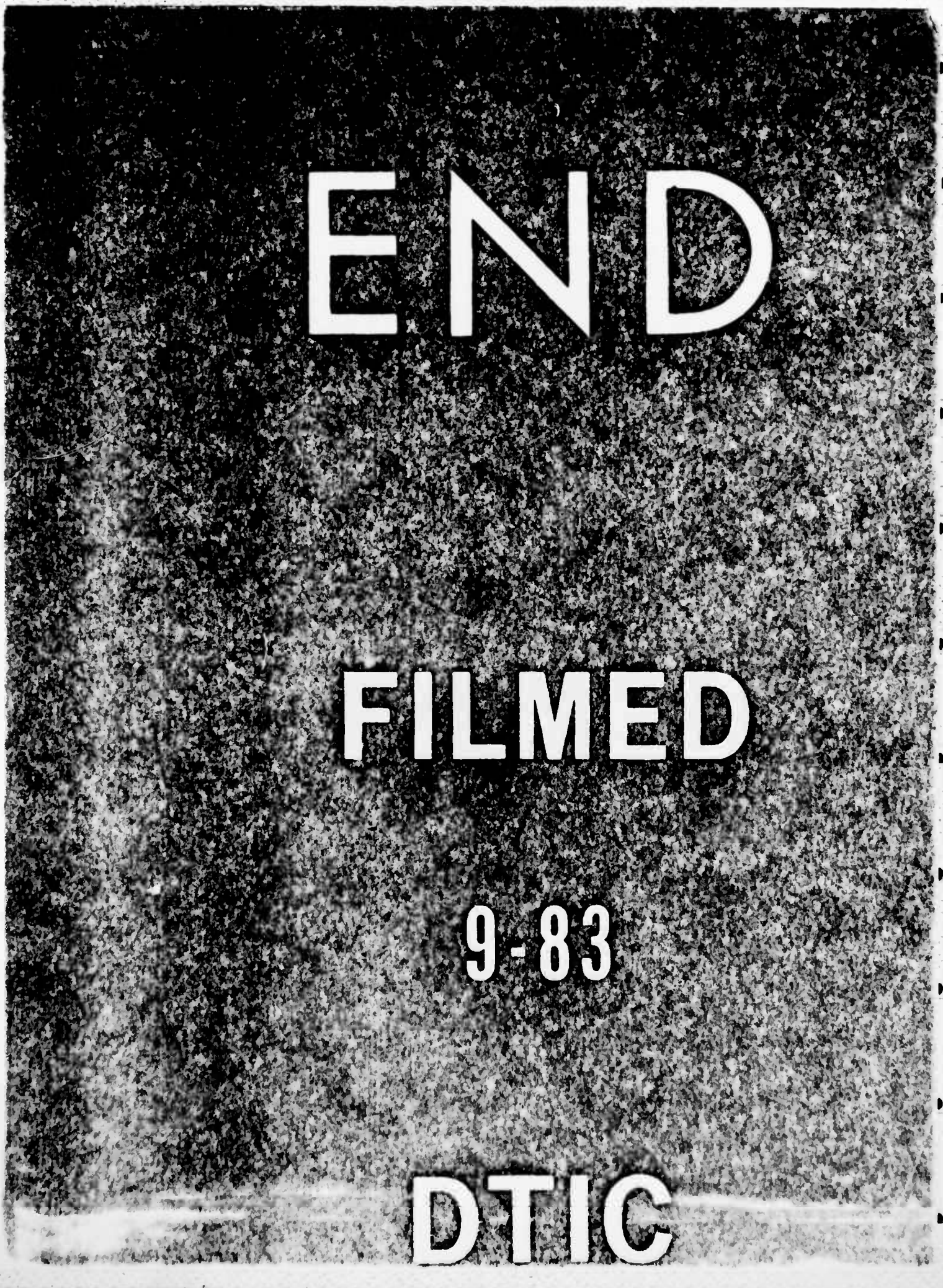
END
FILMED
9-83
DTIC